

THE SMOOTH Mg II GAS DISTRIBUTION THROUGH THE INTERSTELLAR/EXTRA-PLANAR/HALO INTERFACE

GLENN G. KACPRZAK^{1,2}, JEFF COOKE¹, CHRISTOPHER W. CHURCHILL³, EMMA V. RYAN-WEBER¹, AND NIKOLE M. NIELSEN³

ApJL: Accepted Sept. 26, 2013

ABSTRACT

We report the first measurements of Mg II absorption systems associated with spectroscopically confirmed $z \sim 0.1$ star-forming galaxies at projected distances of $D < 6$ kpc. We demonstrate the data are consistent with the well known anti-correlation between rest-frame Mg II equivalent width, $W_r(2796)$, and impact parameter, D , represented by a single log-linear relation derived by Nielsen et al. (MAGII-CAT) that converges to $\sim 2 \text{ \AA}$ at $D = 0$ kpc. Incorporating MAGII-CAT, we find that the halo gas covering fraction is unity below $D \sim 25$ kpc. We also report that our $D < 6$ kpc absorbers are consistent with the $W_r(2796)$ distributions of the Milky Way interstellar medium (ISM) and ISM+halo. In addition, quasar sight-lines of intermediate redshift galaxies with $6 < D < 25$ kpc have an equivalent width distribution similar to that of the Milky Way halo, implying that beyond ~ 6 kpc, quasar sight-lines are likely probing halo gas and not the ISM. As inferred by the Milky Way and our new data, the gas profiles of galaxies can be fit by a single log-linear $W_r(2796) - D$ relation out to large scales across a variety of gas-phase conditions and is maintained through the halo/extra-planar/ISM interfaces, which is remarkable considering their kinematic complexity. These low redshift, small impact parameter absorption systems are the first steps to bridge the gap between quasar absorption-line studies and HI observations of the CGM.

Subject headings: galaxies: halos — galaxies: intergalactic medium — quasars: absorption lines

1. INTRODUCTION

Metal enrichment and the interplay between galaxies and their extra-planar/halo gas is strongly influenced by mergers, galactic winds, high velocity clouds (HVCs), and filamentary infall (see reviews by Putman et al. 2012; Sancisi et al. 2008; Veilleux et al. 2005). However, we lack a thorough understanding of how these processes affect galaxies, their extra-planar gas, and their surrounding circumgalactic medium (CGM). Observation of the quantity, distribution and properties of gas within galaxies and their halos can provide vital insight into the physical processes that govern the dynamics and chemical enrichment of galaxies and the CGM.

The Mg II $\lambda\lambda 2796, 2803$ absorption doublet, detected in background quasar spectra and known to arise from the gaseous halos of galaxies, is an ideal tracer of low-ionization gas with $10^{16} \leq N(\text{HI}) \leq 10^{22} \text{ cm}^{-2}$ (Churchill et al. 2000a; Rigby, Charlton, & Churchill 2002; Churchill, Kacprzak, & Steidel 2005). The combination of the quasar absorption-line technique and a sensitive CGM tracer provides a unique means of directly observing the interplay and mechanisms by which galaxies acquire, expel, chemically enrich, and recycle their gaseous component. Furthermore, a significant quantity of HI is probed by Mg II absorption; roughly equivalent to 5% of the total hydrogen in stars (Kacprzak & Churchill 2011; Ménard & Fukugita 2012).

Although there is significant evidence suggesting that Mg II absorption traces outflows from star-forming galaxies (Bouché et al. 2006; Tremonti et al. 2007; Zibetti et al. 2007; Noterdaeme et al. 2010; Rubin et al. 2010; Bordoloi et al. 2011; Ménard & Fukugita 2012; Martin et al. 2012;

Rubin et al. 2013), accretion onto galaxies (Steidel et al. 2002; Chen et al. 2010; Kacprzak et al. 2010a, 2011b; Ribaud et al. 2011; Churchill et al. 2012; Kacprzak et al. 2012; Martin et al. 2012; Churchill et al. 2013a; Rubin et al. 2013) and high velocity clouds (Richter 2012), with all indicating inclination and azimuthal angle dependencies (Kacprzak et al. 2011b, 2012; Bordoloi et al. 2011, 2012; Bouché et al. 2012), the Mg II rest-frame equivalent width is strongly anti-correlated with impact parameter (e.g., Steidel 1995; Bouché et al. 2006; Kacprzak et al. 2008; Chen et al. 2010; Churchill et al. 2013a; Nielsen et al. 2012, 2013).

With 182 galaxies having impact parameters of $D \gtrsim 10$ kpc, Nielsen et al. (2012, 2013) showed a 7.9σ anti-correlation between $W_r(2796)$ and D . However, it is unclear how this relationship behaves below $D \sim 10$ kpc given that within this regime resides the boundaries between the extended halo gas, the extra-planar gas, HVCs, and the interstellar medium of the host galaxy. Although the $W_r(2796) - D$ relation is smooth, there exists considerable scatter in the data that could be related to the host galaxy luminosity, mass, star formation, orientation, or to a patchy CGM distribution (see Nielsen et al. 2012; Churchill et al. 2013a,b, and references therein). At low impact parameters, the gas covering fraction is expected to be unity (Nielsen et al. 2013) since local HI observations show a unity gas covering fraction within a few kiloparsecs (Zwaan et al. 2005).

In the local Universe, there is a wealth of HI emission-line studies examining the complex extra-planar gas dynamics within 15 kpc of galaxies (limited to $\log N(\text{HI}) < 19$) (Putman et al. 2012; Sancisi et al. 2008; Veilleux et al. 2005). Given that the majority of the gas physics occurs near/above the plane of the disk, it is critical to identify absorption-line systems at low D to examine how the $W_r(2796) - D$ relation behaves around the disk/extra-planar/halo gas interface. Furthermore, absorption systems at $z \sim 0.1$ (e.g., Barton & Cooke 2009) will provide overlapping and complementary data for future HI surveys using The Australian

¹ Swinburne University of Technology, Victoria 3122, Australia
gkacprzak@astro.swin.edu.au

² Australian Research Council Super Science Fellow

³ New Mexico State University, Las Cruces, NM 88003

TABLE 1
KECK-I/LRIS QUASAR/GALAXY OBSERVATIONS

ID	SDSS Quasar Name	z_{qso}	RA (J2000)	DEC (J2000)	θ (")	D (kpc)	z_{gal}	z_{abs}	$W_r(2796)$ (Å)	$W_r(2803)$ (Å)
12	J100514.20+530240.0	0.561	10:05:14.19	+53:02:40.39	0.98 ± 0.04	2.36 ± 0.10	0.1358	0.135215	2.46 ± 0.16	2.24 ± 0.14
16	J110735.68+060758.6	0.380	11:07:35.68	+06:07:58.62	1.52 ± 0.01	4.06 ± 0.03	0.1545	0.154217	3.11 ± 0.32	2.61 ± 0.31
19	J123844.79+105622.2	1.304	12:38:44.79	+10:56:22.23	0.55 ± 0.02	1.18 ± 0.04	0.1185	0.116537	1.75 ± 0.53	2.51 ± 0.40
17	J143458.04+504118.6	1.485	14:34:58.06	+50:41:18.93	1.61 ± 0.09	5.30 ± 0.30	0.1992	0.198697	2.94 ± 0.20	2.91 ± 0.19
14	J145240.54+544345.3	1.519	14:52:40.54	+54:43:45.34	0.62 ± 0.10	1.17 ± 0.19	0.1020	0.101963	2.13 ± 0.49	2.33 ± 0.41
21	J145938.49+371314.7	1.219	14:59:38.49	+37:13:14.69	1.31 ± 0.09	3.40 ± 0.23	0.1489	0.148484	2.16 ± 0.24	1.93 ± 0.20
7	J160521.27+510740.8	1.229	16:05:21.27	+51:07:41.29	2.12 ± 0.08	3.90 ± 0.15	0.0994	0.098006	2.35 ± 0.38	2.68 ± 0.22

Square Kilometer Array Pathfinder, such as WALLABY (600k galaxies at $z = 0 - 0.25$) and DINGO (100k galaxies at $z = 0 - 0.40$).

Motivated by the lack of overlap between H I emission and absorption-line system observations and the lack of absorption-line systems within this low impact parameter range, we identified seven new Mg II absorbers with $D < 6$ kpc. These observations provide the first glimpses into the galaxy/extra-planar/halo gas boundaries connecting H I and Mg II observations. In § 2 we describe our sample selection and analysis. In § 3, we present the $D < 6$ kpc absorbers and how they fit on the existing $W_r(2796) - D$ anti-correlation. We further compare our systems to those in our own Milky Way in order to interpret the plausible origin of the absorbing gas at very small impact parameters. Our concluding remarks are in § 4. We adopt a $h = 0.70$, $\Omega_M = 0.3$, $\Omega_\Lambda = 0.7$ cosmology.

2. THE SAMPLE AND ANALYSIS

The Sloan Digital Sky Survey (SDSS) spectroscopic fibers have a diameter of $3''$ (8 kpc at $z = 0.15$), thus, any fiber could contain a background quasar and a foreground galaxy. Therefore close star-forming galaxy and quasar pairs can be identified by quasar spectra having superimposed foreground galaxy emission-line spectra. York et al. (2012) identified 23 H α -emitting foreground galaxies with $z < 0.4$ at small impact parameters from quasars using the SDSS Data Release 5 and Noterdaeme et al. (2010) identified 46 [O III]-emitting galaxies at $z < 0.8$ within the SDSS Data Release 7. Here we have identified a subset of seven $z \sim 0.1$ galaxies that are clearly identified in ground-based imaging and are at a redshift where it is possible to detect their Mg II absorption using blue sensitive optical CCDs (see Barton & Cooke 2009).

2.1. Quasar Spectroscopy

The seven quasar spectra were obtained on 2013 April 10 using the Keck Low Resolution Imaging Spectrometer (LRIS) (Oke et al. 1995) with the 1200 lines/mm grism blazed at 3400 \AA , which covers a wavelength range of $2910 - 3890 \text{ \AA}$. We used a $0.7''$ slit ($1''$ slit for ID7), providing a dispersion of 0.17 \AA per pixel and a resolution of $\sim 1.12 \text{ \AA}$ ($\sim 105 \text{ km s}^{-1}$). Integration times of 2200–4400 seconds were used, depending on the magnitude of the quasar and the foreground galaxy redshift. The spectra were reduced using the standard IRAF packages and were heliocentric and vacuum corrected.

The quasar spectra were objectively searched for Mg II doublet candidates using a detection significance level of 3σ (2σ for ID19) for the $\lambda 2796$ and $\lambda 2803$ lines. All seven absorbers are also identifiable by their strong Mg I $\lambda 2853$ absorption. Detection and significance levels follow the formalism of Churchill et al. (1999). Analysis of the absorption profiles was performed using our own graphic-based interac-

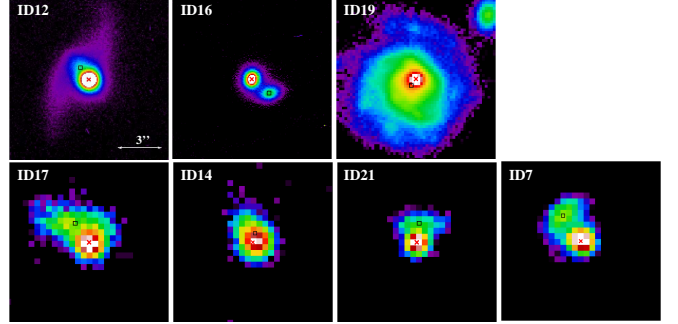


FIG. 1.— $15 \times 15''$ images (27.7×27.7 kpc at $z = 0.1$) of the obscured quasar (center indicated by an “X”) and the emission-line foreground galaxies (centers indicated by an square) producing the observed Mg II absorption. The close galaxy and quasar pairs were identified by the quasar spectra having superimposed foreground galaxy emission-line spectra. The top panels are Gemini/GMOS-N i -band, Gemini/GMOS-S i -band and CFHT/MegaPrime g -band images (left to right). The bottom panels are SDSS r -band images.

tive software that uses the direct pixel values to measure the equivalent widths and the redshift of the Mg II $\lambda 2796$ transition. The Mg II absorption redshifts were computed from the optical depth weighted mean of the absorption profiles (see Churchill & Vogt 2001). The statistical redshift uncertainties range between $0.00001 - 0.00009$ ($\sim 3 - 30 \text{ km s}^{-1}$ comoving).

2.2. Galaxy/Quasar Imaging

In Figure 1, we present the seven new quasar-galaxy pairs where the quasar is placed in the center of the image. All galaxies were imaged with SDSS ($0.4''/\text{pixel}$), however additional archival imaging was obtained for three of the objects from the Canadian Astronomy Data Centre (CADC). ID12 was imaged on 20 December 2008 for 1100 seconds using Gemini/GMOS-N ($0.073''/\text{pixel}$) in the i -band (PID GN-2008B-Q-128), ID16 was imaged on 27 December 2008 for 1100 seconds using Gemini/GMOS-S ($0.073''/\text{pixel}$) in the i -band (PID GS-2008B-Q-79) and ID19 was imaged on 25 May 2009 for 3171 seconds using CFHT/MegaPrime ($0.19''/\text{pixel}$) in the g -band (PID 09AP03).

Impact parameters were computed between the photometric centroids of the background quasar and galaxy using Source Extractor (Bertin & Arnouts 1996). In cases where the quasar and galaxy are blended (e.g., ID14), we performed a PSF subtraction of the quasar light. The PSFs were created by modeling selected stars within the same field.

3. RESULTS & DISCUSSION

In Table 1 we present seven new $z \sim 0.1$ Mg II absorption systems that have measured rest-frame equivalent widths in the range of $1.75 \leq W_r(2796) \leq 3.11 \text{ \AA}$. The absorbers are detected within $1.17 \leq D \leq 5.30$ kpc of their host galaxies and

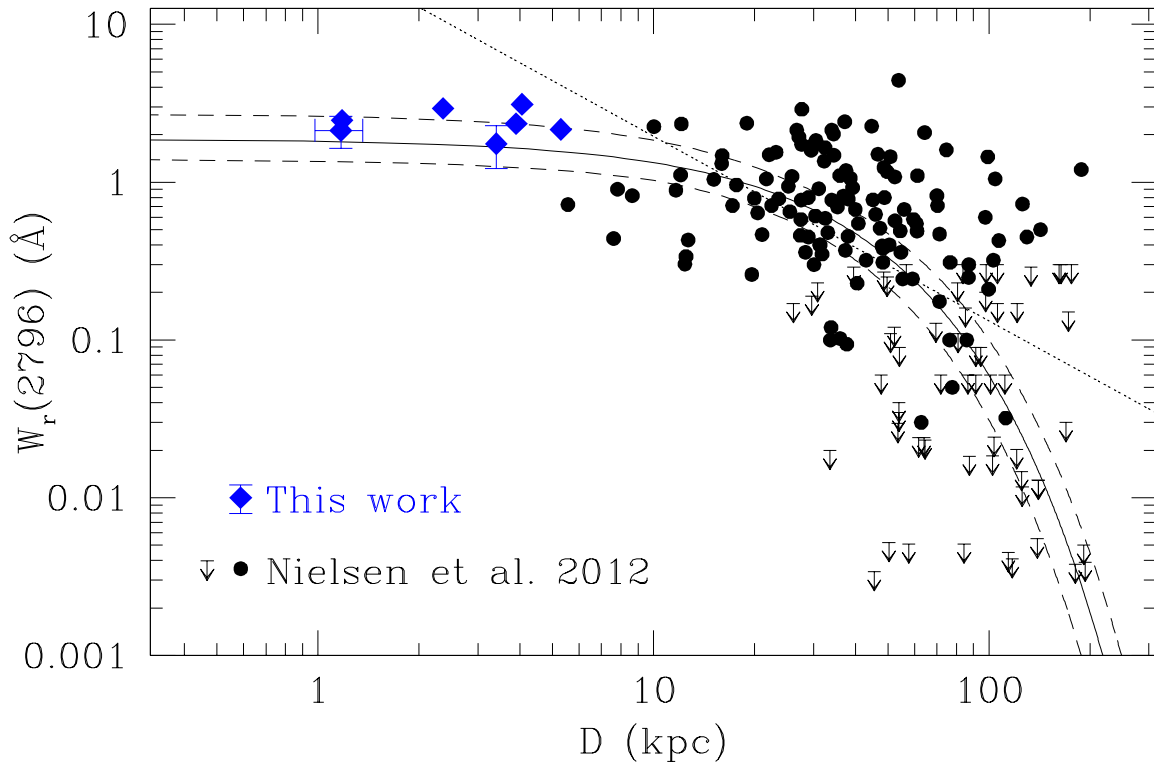


FIG. 2.— The MgII $\lambda 2796$ rest-frame equivalent width, $W_r(2796)$, versus impact parameter, D . Galaxies with detected MgII absorption are presented as filled point-types while those with upper limits are indicated with downward arrows. The circles and arrows represent the MAGIIICAT sample comprising 182 galaxies and the solid line is a maximum likelihood log-linear fit where $\log[W_r(2796)] = (-0.015 \pm 0.002) \times D + (0.27 \pm 0.11)$ and the dashed curves provide 1σ uncertainties (Nielsen et al. 2012, 2013). The dotted line is the power-law fit derived by Chen et al. (2010). Our new objects have $D < 6$ kpc and are indicated with blue diamonds.

have relative velocity offsets of $10 \leq \Delta v \leq 530 \text{ km s}^{-1}$. A detailed kinematics study will be presented in an upcoming paper. The host galaxies have a $\langle L_R \rangle = 0.5 L_*$ and a $\langle \text{SFR} \rangle = 2 M_\odot \text{ yr}^{-1}$ (York et al. 2012). These systems represent the lowest impact parameters probing MgII absorption around known host galaxies. At these projected separations we are likely probing HI column densities of $\log[N(\text{HI})] \sim 19-21$ that are typically detected around local star-forming galaxies and extend out to 10–15 kpc (see Sancisi et al. 2008).

In Figure 2 we show the current state of the $W_r(2796) - D$ relation for known MgII absorption systems that are associated with spectroscopically identified host galaxies. The circles and limits represent a body of work from the literature consisting of 182 absorbers and non-absorbers, respectively, recently compiled in the MAGIIICAT⁴ (Nielsen et al. 2012, 2013). For our analysis, we have added an additional MAGIIICAT galaxy to our $D < 6$ kpc sample that is associated with a $W_r(2796) = 0.72 \text{ \AA}$ absorber at $D = 5.4$ kpc (Steidel et al. 1993; Guillemin & Bergeron 1997). Nielsen et al. (2012) found a 7.9σ anti-correlation between D and $W_r(2796)$ that is best fit by $\log[W_r(2796)] = (-0.015 \pm 0.002) \times D + (0.27 \pm 0.11)$. The dotted line is a power-law fit by Chen et al. (2010) to a subset of 71 systems.

Our seven new absorbers are presented as diamonds (blue) in Figure 2. We find that the Chen et al. (2010) extrapolated fit over-estimates the expected equivalent widths at low impact parameters. However, we find that the eight $D < 6$ kpc absorbers follow the MAGIIICAT fit, even around ~ 1 kpc. This is interesting since MgII absorption at higher impact

parameters is expected to trace a range of kinematically different, infalling, outflowing, metal-poor, metal-rich gas structures, while gas within a few kiloparsecs should be associated with an extended, infalling, and co-rotating extra-planar disk (e.g., Fraternali et al. 2002; Heald et al. 2007) combined with possible wind signatures (e.g., Martin et al. 2012; Rubin et al. 2013). Therefore it is interesting that, to first order, the equivalent widths, which measure both gas kinematics and quantity, exhibit a smooth continuity with the log-linear fit based upon extended halo gas. This may reflect recent results that MgII gaseous halos are self-similar when normalized by the galaxy halo mass, indicating that regardless of the kinematic and gas origins, the halo mass is the dominant driving factor in determining their properties (Churchill et al. 2013a,b). The smooth $W_r(2796) - D$ relation does not necessarily imply that the gas distribution within an individual galaxy is smooth, but rather that gas patchiness and kinematic/column density profiles conspire to yield a monotonically decrease gas profile for a heterogeneous population of galaxies with random orientations.

The halo gas covering fraction is found to be unity within 10 kpc, which is consistent with the unity HI emission covering fraction for local star-forming galaxies out to 10 kpc (see Sancisi et al. 2008). The eight absorbers within 6 kpc have a mean $\langle W_r(2796) \rangle = 2.2 \text{ \AA}$; using the Ménard & Chelouche (2009) $N(\text{HI}) - W_r(2796)$ relation this translates to $\log[N(\text{HI})] \sim 20.1$, the typical column density of DLAs/sub-DLAs at $D \sim 7$ kpc of galaxy disks (Zwaan et al. 2005). In addition, the covering fraction remains unity out to 25 kpc. Our eight galaxies are expected to contain a significant HI gas component since they were selected by emission

⁴ <http://astronomy.nmsu.edu/cwc/Group/magiiicat/>

lines produced by ongoing star formation.

Given that the $W_r(2796)$ distribution is roughly constant within 10 kpc, with unity covering fraction, we can assume that the column density profile is roughly constant towards the galaxy center with $\langle \log[N(\text{H I})] \rangle \sim 20.1$ (for $\langle W_r(2796) \rangle = 2.2 \text{ \AA}$). The product of the column density and a gas cross-section of radius 10 kpc yields an estimated total H I mass traced by Mg II of $M_{\text{H I}} = 1.3 \times 10^8 M_{\odot}$. The eight galaxies in our analysis have a mean luminosity of $\langle L_R \rangle = 0.5 L_*$ and are expected to have a typical total H I gas mass of $M_{\text{H I}} \sim 5 \times 10^9 - 2 \times 10^{10} M_{\odot}$ (Huang et al. 2012). Our derived H I mass is consistent with the expected halo/extraplanar H I gas mass, which are roughly 1–30% of the total H I gas mass (Sancisi et al. 2008). However, since the quasar lines-of-sight pass very near to and through the galaxy disk, it is expected that the computed H I mass traced by Mg II absorption is equivalent to the total expected H I mass. This H I mass inconsistency could be caused by: (1) the $N(\text{H I})-W_r(2796)$ relation under-predicting the amount of H I at high $W_r(2796)$, (2) the Mg II absorption tracing only halo/extraplanar material outside the higher column density disk, or (3) the $W_r(2796)-D$ relation having a sharp turn-up in equivalent width at D smaller than we have probed with this work in order to account for the remaining missing gas mass.

Zwaan et al. (2005) reproduced the incidence rate of high redshift DLAs assuming that DLAs arise from disk/ISM gas of local galaxies and found that the median D giving rise to DLAs was 7.3 kpc; we apply this D -cut which is equivalent to a $D < 6$ kpc cut for our study (see Figure 2). To examine if the equivalent widths found for the $D < 6$ kpc sight-lines are representative of a combination of halo gas and the interstellar medium (ISM), we use the best studied case – the Milky Way (MW). The most comprehensive absorption-line analysis of the MW was performed by the Hubble Space Telescope Quasar Absorption Line Key Project (Bahcall et al. 1993). A total of 83 quasars were observed with the Faint Object Spectrograph G190H and G270H gratings identifying 85 Galactic Mg II systems: 71 Mg II systems are identified as being free of IGM Ly α contamination from high redshift sources (Savage et al. 2000). Savage et al. (2000) identified 71 systems as being ISM+HVC/halo gas (see their Table 7, columns 8+10) and 21 systems as HVC/halo gas (see their Table 7, column 10). We do not attempt to differentiate between absorption produced by HVCs or halo gas, so we adopt the notation of “MW ISM+halo” and “MW halo” absorption systems. Although this is the best sample to compare to, there is one caveat: the MW sight-lines pass through approximately half of the disk/halo. Accounting for the highly saturated nature of the MW absorption-lines, and assuming the gas velocity dispersion is symmetric about the disk-plane, we multiply the equivalent widths by a factor of two to emulate a full line-of-sight through the MW.

In Figure 3, we plot the equivalent width distributions of the $D < 6$ kpc sample and MW ISM+halo sample. Note that the $D < 6$ kpc and the MW ISM+halo samples are similar with median values of 2.25 \AA and 2.70 \AA and average values of 2.20 \AA and 2.70 \AA , respectively. A Kolmogorov-Smirnov (KS) test indicates that the $D < 6$ kpc and the MW ISM+halo $W_r(2796)$ distributions are likely drawn from the same parent population with $P(KS) = 0.576$ (0.80σ). This implies that the $D < 6$ kpc sample is likely detecting the expected total ISM+halo of their host galaxies. Given that the MW ISM+halo $W_r(2796)$ distribution is consistent with the

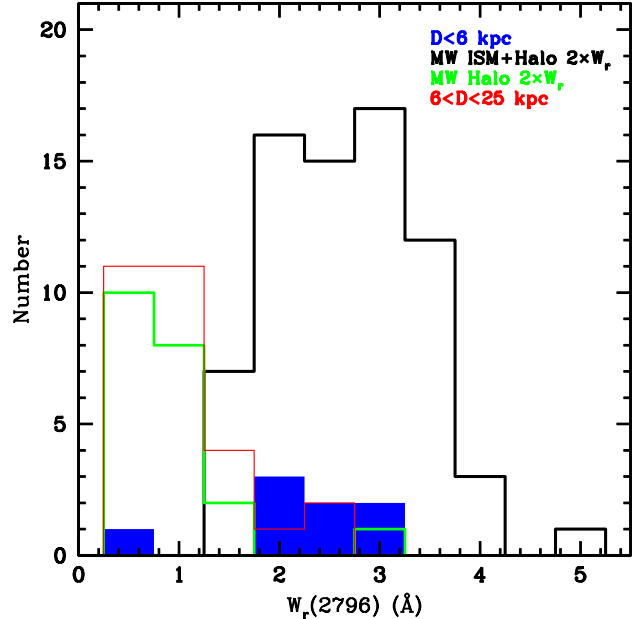


FIG. 3.— The Mg II $\lambda 2796$ rest-frame equivalent width, $W_r(2796)$, distributions are shown for the $D < 6$ kpc (blue) and the $6 < D < 25$ kpc (red) quasar absorption-line systems. A comparison is made between intermediate redshift systems and those through the Milky Way (MW). A correction factor of two is applied since sight-lines are intercepted halfway through the disk/halo. The $W_r(2796)$ distributions of the the MW ISM+halo (black) and the halo (green) are shown. Note the $D < 6$ kpc systems and those of the MW ISM+halo systems have similar distributions. The $6 < D < 25$ kpc systems have a similar distribution to the MW halo.

$D < 6$ kpc distribution, and that the ISM will unlikely produce higher $W_r(2796)$ systems, we would not expect to observe a sharp upturn in the $W_r(2796)-D$ relation as one approaches $D = 0$ kpc. Although the sight-lines through the MW intercept the disk at $D = 8.5$ kpc, the H I radial column density profile is rather flat for $D < 8.5$ kpc (Kalberla & Kerp 2009) and the $W_r(2796)$ distribution would likely be similar if we were located elsewhere in the disk.

In Figure 3 we show the $6 < D < 25$ kpc equivalent width distribution for intermediate redshift galaxies from MAGII-CAT. Note that compared to the $D < 6$ kpc sight-lines, they appear quite different with an average $W_r(2796)$ of 1.0 \AA compared to 2.2 \AA ($D < 6$ kpc). A KS test shows that two populations differ at the 3.1 σ level ($P(KS) = 0.002$). We further show the $W_r(2796)$ distribution of MW halo systems in Figure 3, which has an average $W_r(2796)$ of 0.86 \AA . The MW halo distribution is similar to the $6 < D < 25$ kpc distribution with $P(KS) = 0.767$ (1.19σ) and very different from the $D < 6$ kpc distribution at the 3.4 σ level ($P(KS) = 0.00072$). The similar distribution between the MW halo and $6 < D < 25$ kpc systems suggest that higher impact parameter quasar sight-lines systems likely probe halo gas material at much lower H I column densities. Thus, small- D Mg II absorption systems are indeed tracing the ISM or ISM+halo gas from their host galaxies, relative to expectations from the MW.

Our initial H I mass calculation must suffer from geometry and/or filling factor assumptions and/or uncertainties of the $N(\text{H I})-W_r(2796)$ relation (Ménard & Chelouche 2009). The $N(\text{H I})-W_r(2796)$ relation contains scatter over 4 orders of magnitude and DLA column densities exist only for $W_r(2796) > 3 \text{ \AA}$, while DLAs are observed in systems as low as 0.6 \AA (Rao et al. 2006). Although this relation provides an

indirect means for computing the median $N(\text{H I})$, it may have limitations.

4. CONCLUSION

We have obtained the first measurements of Mg II absorption associated with spectroscopically confirmed star-forming galaxies at projected distances of $D < 6$ kpc. We find the following:

1. The well known anti-correlation between rest-frame Mg II equivalent width and impact parameter is maintained for systems with $0.5 < D < 6$ kpc and the gaseous halos have unity covering fraction within $D < 25$ kpc. Furthermore, the $W_r(2796)$ relation converges to $\sim 2 \text{ \AA}$ at $D = 0$ kpc.
2. When compared to the Milky Way, we find that our $D < 6$ kpc sample is consistent with the $W_r(2796)$ distributions of the MW ISM+halo; the majority of the $W_r(2796)$ is produced by the ISM. This indicates that our new systems are likely probing the ISM/disk and halo gas of their host galaxies.
3. The comparison between the MW and small- D absorption-line systems indicates that the halo gas profile likely decreases monotonically from the galaxy center out to ~ 150 kpc, with the covering fraction decreasing as a function of D . This implies no rapid increase in $W_r(2796)$ at D approaches 0 kpc. Our data show there is a smooth log-linear continuity in the gas content from the outer halo all the way to the halo/extrplanar/ISM interface of galaxies and is not in agreement

with the extrapolations of power-law fit of (Chen et al. 2010).

4. When compared to the MW, quasar sight-lines with $6 < D < 25$ kpc have a $W_r(2796)$ distribution similar to that of MW halos, implying that beyond $D \sim 6$ kpc, quasar sight-lines likely are tracing halo gas only.

It is remarkable that gas profiles of galaxies can be fit by a single log-linear $W_r(2796) - D$ relation over such large scales and range of gas-phase conditions. Consistent with the MW, this relation is maintained through the halo/extra-planar/ISM interfaces regardless of their complex kinematic interplay. This further implies a smooth H I column density profile surrounding galaxies below current observational limits.

These low redshift, small- D absorption systems will be important in bridging the gap between absorption-line studies and future H I observations/surveys, which could play a key role in understanding the CGM.

ERW acknowledges Australian Research Council grant DP 1095600. CWC was partially supported through the Research Enhancement Program from NASA's New Mexico Space Grant Consortium. NMN was partially support through an NSF EAPSI grant and a GREG at NMSU. Data was obtained at the W.M. Keck Observatory, which is operated as a scientific partnership among the California Institute of Technology, the University of California and the National Aeronautics and Space Administration. The Observatory was made possible by the generous financial support of the W.M. Keck Foundation. Data was also obtained from The Sloan Digital Sky Survey (SDSS/SDSS-II), which is funded by the Alfred P. Sloan Foundation, Participating Institutions, NSF, U.S. Department of Energy, NASA, Japanese Monbukagakusho, Max Planck Society, and the Higher Education Funding Council for England.

Facilities: Keck I (LRIS), Sloan (SDSS).

REFERENCES

- Bahcall, J. N., Bergeron, J., Boksenberg, A., et al. 1993, *ApJS*, 87, 1
 Barton, E. J., & Cooke, J. 2009, *AJ*, 138, 1817
 Bordoloi, R., Lilly, S. J., Kacprzak, G. G., & Churchill, C. W. 2012, arXiv:1211.3774
 Bordoloi, R., Lilly, S. J., Knobel, C., et al. 2011, *ApJ*, 743, 10
 Bertin, E., & Armouts, S. 1996, *A&AS*, 117, 393
 Bouché, N., Hohensee, W., Vargas, R., Kacprzak, G. G., et al. 2012, *MNRAS*, 426, 801
 Bouché, N., Murphy, M. T., Péroux, C., Csabai, I. & Wild. V. 2006 *MNRAS*, 371, 495
 Chen, H.-W., Helsby, J. E., Gauthier, J.-R., Shtetman, S. A., Thompson, I. B., & Tinker, J. L. 2010a, *ApJ*, 714, 1521
 Churchill, C. W., Kacprzak, G. G., & Steidel, C. C. 2005, in *Probing Galaxies through Quasar Absorption Lines*, IAU 199 Proceedings, eds. P. R. Williams, C.-G. Shu, & B. Ménard (Cambridge: Cambridge University Press), p. 24
 Churchill, C. W., Kacprzak, G. G., Steidel, C. C., et al. 2012, *ApJ*, 760, 68
 Churchill, C. W., Mellon, R. R., Charlton, J. C., Jannuzi, B. T., Kirhakos, S., Steidel, C. C., & Schneider, D. P. 2000a, *ApJS*, 130, 91
 Churchill, C. W., Nielsen, N. M., Kacprzak, G. G., & Trujillo-Gomez, S. 2013, *ApJ*, 763, L42
 Churchill, C. W., Rigby, J. R., Charlton, J. C., & Vogt, S. S. 1999, *ApJS*, 120, 51
 Churchill, C. W., Trujillo-Gomez, S., Nielsen, N. M., & Kacprzak, G. G. 2013, arXiv:1308.2618
 Churchill, C. W., & Vogt, S. S. 2001, *AJ*, 122, 679
 Fraternali, F., van Moorsel, G., Sancisi, R., & Oosterloo, T. 2002, *AJ*, 123, 312
 Guillemin p., & Bergeron, J. 1997, *A&A*, 328, 499
 Heald, G. H., Rand, R. J., Benjamin, R. A., & Bershady, M. A. 2007, *ApJ*, 663, 933
 Huang, S., Haynes, M. P., Giovanelli, R., et al. 2012, *AJ*, 143, 133
 Kacprzak, G. G., & Churchill, C. W. 2011c, *ApJ*, 743, L34
 Kacprzak, G. G., Churchill, C. W., Ceverino, D., Steidel, C. C., Klypin, A., & Murphy, M. T. 2010a, *ApJ*, 711, 533
 Kacprzak, G. G., Churchill, C. W., Evans, J. L., Murphy, M. T., & Steidel, C. C. 2011b, *MNRAS*, 416, 3118
 Kacprzak, G. G., Murphy, M. T., & Churchill, C. W. 2010b, *MNRAS*, 406, 445
 Kacprzak, G. G., Churchill, C. W., Steidel, C. C., & Murphy, M. T. 2008, *AJ*, 135, 922
 Kacprzak, G. G., Churchill, C. W., Steidel, C. C., Spitler, L. R., & Holtzman, J. A. 2012, *MNRAS*, 427, 3029
 Kalberla, P. M. W., & Kerp, J. 2009, *ARA&A*, 47, 27
 Martin, C. L., Shapley, A. E., Coil, A. L., et al. 2012, *ApJ*, 760, 127
 Ménard, B., & Chelouche, D. 2009, *MNRAS*, 393, 808
 Ménard, B., & Fukugita, M. 2012, *ApJ*, 754, 116
 Oke, J. B., et al. 1995, *PASP*, 107, 375
 Nielsen, N. M., Churchill, C. W., & Kacprzak, G. G. 2012, arXiv:1211.1380
 Nielsen, N. M., Churchill, C. W., Kacprzak, G. G., & Murphy, M. T. 2013, arXiv:1304.6716
 Noterdaeme, P., Srianand, R., & Mohan, V. 2010, *MNRAS*, 403, 906
 Putman, M. E., Peek, J. E. G., & Jounge, M. R. 2012, *ARA&A*, 50, 491
 Rao, S. M., Turnshek, D. A., & Nestor, D. B. 2006, *ApJ*, 636, 610
 Ribado, J., Lehner, N., Howk, J. C., et al. 2011, *ApJ*, 743, 207
 Richter, P. 2012, *ApJ*, 750, 165
 Rigby, J. R., Charlton, J. C., & Churchill, C. W. 2002, *ApJ*, 565, 743
 Rubin, K. H. R., Prochaska, J. X., Koo, D. C., et al. 2013, arXiv:1307.1476
 Rubin, K. H. R., Prochaska, J. X., Koo, D. C., Phillips, A. C., & Weiner, B. J. 2010, *ApJ*, 712, 574
 Sancisi, R., Fraternali, F., Oosterloo, T., & van der Hulst, T. 2008, *A&A Rev.*, 15, 189

- Savage, B. D., Wakker, B., Jannuzi, B. T., et al. 2000, *ApJS*, 129, 563
- Steidel, C. C. 1995, in *QSO Absorption Lines*, ed. G. Meylan, (Springer-verlag: Berlin Heidelberg), p. 139
- Steidel, C. C., Dickinson, M., & Bowen, D. V. 1993, *ApJ*, 413, L77
- Steidel, C. C., Kollmeier, J. A., Shapely, A. E., Churchill, C. W., Dickinson, M., & Pettini, M. 2002, *ApJ*, 570, 526
- Tremonti, C. A., Moustakas, J., & Diamond-Stanic, A. M. 2007, *ApJ*, 663, L77
- Veilleux, S., Cecil, G., & Bland-Hawthorn, J. 2005, *ARA&A*, 43, 769
- York, D. G., Straka, L. A., Bishof, M., et al. 2012, *MNRAS*, 423, 3692
- Zibetti, S., Ménard, B., Nestor, D. B., Quider, A. M., Rao, S. M., & Turnshek, D. A. 2007, *ApJ*, 658, 161
- Zwaan, M. A., van der Hulst, J. M., Briggs, F. H., Verheijen, M. A. W., & Ryan-Weber, E. V. 2005, *MNRAS*, 364, 1467